
Autonomous navigation in urban areas using GIS-managed information

Philippe Bonnifait,* Maged Jabbour and
Véronique Cherfaoui

Heudiasyc UMR CNRS 6599,
Université de Technologie de Compiègne,
BP 20529, Compiègne, cedex 60205 France
E-mail: Philippe.Bonnifait@hds.utc.fr
E-mail: Maged.Jabbour@hds.utc.fr
E-mail: Veronique.Cherfaoui@hds.utc.fr
*Corresponding author

Abstract: This paper describes the usefulness of a Geographical Information System (GIS) for autonomous navigation of intelligent vehicles. In many urban applications the use of GPS alone is not sufficient and needs to be backed up with Dead-Reckoned (DR) sensors, map data and additional sensors like cameras or laser scanners. Geographical information can be used in two different ways. Firstly, preexisting features of the environment, such as roads, can be used as constraints in localisation space. Secondly, the geographical information can include landmark locations. The use of these two types of data is illustrated by a localisation system for urban areas: a laser scanner detects natural landmarks that are characterised during a learning phase. As the amount of data can be large, we propose a strategy for grouping the laser landmarks in enhanced local maps corresponding to the roads of a GIS layer, through the use of an L1 GPS receiver and DR sensors. Real experiments are reported to illustrate the performance of this approach.

Keywords: urban localisation; natural landmarks; geographical information system; GIS; GPS.

Reference to this paper should be made as follows: Bonnifait, P., Jabbour, M. and Cherfaoui, V. (2008) 'Autonomous navigation in urban areas using GIS-managed information', *Int. J. Vehicle Autonomous Systems*, Vol. 6, Nos. 1/2, pp.83–103.

Biographical notes: Philippe Bonnifait graduated from the Ecole Supérieure d'Électronique de l'Ouest, France, and received a PhD in Automatic Control and Computer Science from the Ecole Centrale de Nantes, France. He also received the Habilitation à Diriger des Recherches from the Université de Technologie de Compiègne (UTC) and was with Heudiasyc. He is a Professor at the UTC, Department of Computer Science and Engineering. His current research interests are in intelligent vehicles and advanced driving assistance systems, with particular emphasis on dynamic ego-localisation based on multisensor-fusion (GNSS, dead-reckoning and GIS).

Maged Jabbour graduated from the Faculty of Engineering of the Lebanese University in 2003 with a Master's degree in Electrical and Electronic Engineering. In 2004, he received a Research Master's degree (DEA) in Information and System Technologies from the Université de Technologie de Compiègne (UTC), France. Currently, he is a PhD student at the Université de Technologie de Compiègne (UTC), France.

Véronique Cherfaoui has received an MS in Computer Science from the Lille University, France, in 1988 and a PhD in Control of Systems from the University of Technology of Compiègne, France in 1992. She is an Associate Professor in Department of Computer Engineering at the University of Technology of Compiègne. Her research interests in the Heudiasyc-CNRS laboratory are data fusion algorithms in distributed architecture, data association and perception system for intelligent vehicles.

1 Introduction

Intelligent vehicles are advanced vehicles that can perform driving assistance tasks or autonomous navigation in the presence of uncertainty and variability in their environment. Cybercars are a particular type of intelligent vehicles that can be used in downtown areas as an alternative to private cars for transporting people. This is the Cybernetic Transportation System concept (Parent and Gallais, 2002). Several successful experiments have demonstrated that they can navigate autonomously by sensing dedicated equipment integrated into the urban infrastructure. This equipment includes catadioptric beacons, magnets and wires buried in the road (Georgiev and Allen, 2004). A challenging issue is giving vehicles sufficient autonomy to navigate in unequipped environments using natural landmarks (Kais et al., 2004). One approach to this problem is to start from a precise location and then to control the vehicle's movement with respect to a planned trajectory while detecting obstacles (Vasquez et al., 2004).

Global Navigation Satellite-based Systems (GNSS) like GPS, Glonass and, in the near future, Galileo are very interesting candidates for localisation purposes, since Real Time Kinematic (RTK) GPS can achieve accuracy to within a few centimetres in real time using phase corrections broadcast by base stations. Nevertheless, this technology is not adapted to cybercars moving around in urban areas, since the receiver needs to see at least five satellites with a good configuration (small Dilution of Precision (DOP)). Moreover, after the loss of the RTK mode, the system needs to solve the problem of phase ambiguities, which typically requires 30 sec of processing. Since RTK is unsuitable, one might consider using differential L1 GPS (pseudo-ranges measurements). Unfortunately, the best attainable precision is in the order of 30/50 cm, which is not adapted to the navigation needs of a cybercar.

One solution is to use additional sensors such as video cameras and laser range scanners embedded in the vehicle (Wang et al., 2004). Indeed, they are well adapted to the sensing of natural landmarks, especially in urban settings where landmarks such as buildings and road features are particularly stable. The landmarks are characterised and localised in a learning stage during which the vehicle is driven manually. Afterwards, the vehicle is able to localise itself and control its movement in the vicinity of the learnt trajectory. Recent studies (such as the experiments performed by Royer et al. (2005) using computer vision) have proved the validity of such a concept. One of the difficulties with this approach is the management and the structuring of the large amount of landmark data for online navigation. What is the best way to organise landmark information for a cybercar moving within a large area containing many roads? The usual answer to this question is to group landmarks together in local maps, a local map being a set of landmarks put together because of

- 1 memory constraints arising from the use of embedded systems
- 2 the need to download or update a limited amount of data from a distant server
- 3 the connections that exist between the landmarks, essential for computing a location.

Localisation with respect to a digital map describing the road network is an essential task for cybercars. The user of the vehicle usually specifies its itinerary by indicating the address of the destination, which makes the geocoding facility of Geographical Information Systems (GIS) very useful for converting an address like ‘10, Albert Road’ to a global (x, y) coordinate point.

The GIS can also be used for the management of the landmarks by making use of descriptions of roads in the map database. To achieve this goal, a GNSS receiver is needed. This is useful for the georeferencing of the landmarks characterised during the learning stage, and it is also useful for the extraction of the landmarks during the autonomous navigation stage. For these requirements, the absolute accuracy of GNSS positioning is not crucial since the roadmap has a metre-level precision. Therefore, an L1 (single frequency) GPS receiver backed up by Dead-Reckoned (DR) sensors in order to handle satellite outages is sufficient.

The aim of this paper is to illustrate the use of GIS for autonomous navigation of intelligent vehicles. We present a new strategy for the management of natural landmarks in enhanced local maps stored in a dedicated GIS layer. The precise localisation used to control the vehicle is obtained via a two-level process. First, a coarse localisation uses differential-L1 GPS, odometry aided by a gyrometer and a road map. As a result, the right local map is extracted from the GIS database and then the second localisation stage is performed using natural landmarks detected by a laser scanner in order to increase the precision.

This paper is organised as follows. The following section describes the GIS and the natural urban landmarks. Section 3 presents the coarse localisation method whose goal is to determine the right road. In Section 4, the geo-referencing of the landmarks and their grouping together in local maps is described. In Section 5, the management of landmarks during the navigation stage is performed. The final section is devoted to real experiments carried out with our experimental vehicle.

2 Geographical information

A GIS is a set of tools and methods that manage and handle vectorised or raster geographical information. It also provides tools to extract navigation data, such as road signs or pedestrian crossings, to be used by cybercars. For an autonomous vehicle that navigates in an urban environment, the GIS must be able to handle path planning (destination chosen by the user), map matching, attribute extraction and landmark management for precise navigation purposes.

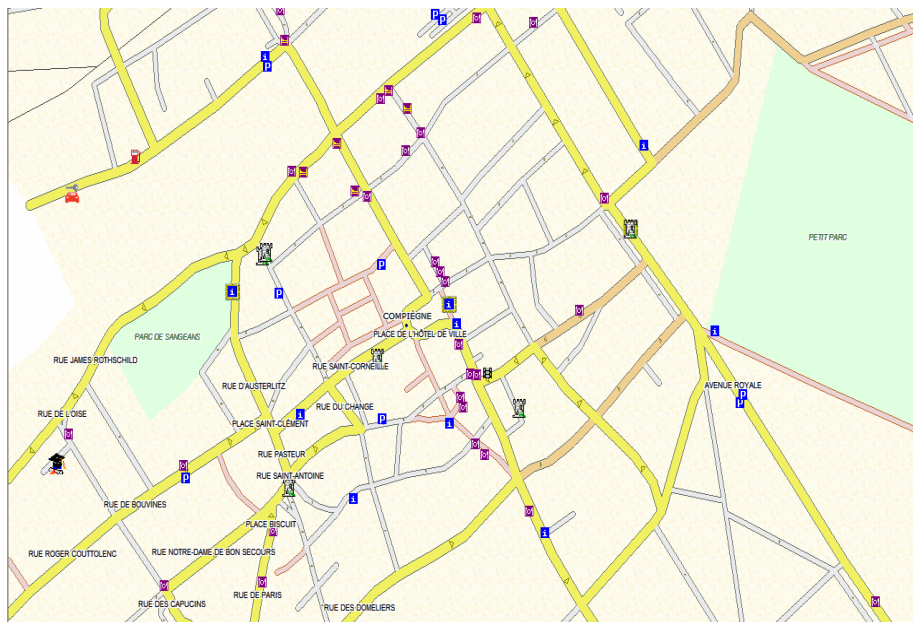
2.1 Road map GIS layer

A GIS map database is usually a set of digitised roads described by poly-lines (see Figure 1) provided by cartographers such as *NavTeQ* or *TeleAtlas*. This topological information is very useful for navigation tasks like path planning. Indeed, for this

purpose, a scanty representation of the road network is sufficient: a road is described by a single line corresponding to its central axis.

The use of this topology is also interesting for the management of landmarks (Kim et al., 2000) and consequently of local maps. Once the location of the vehicle unambiguously map-matches with a road, the pertinent landmarks are those associated with this road. Secondly, if the vehicle is autonomous (i.e. driven by a regulator), it has to follow a predefined trajectory described by a set of connected roads. In this case, the pertinent landmarks are those associated with this path. Therefore, we propose in this work to map-match the landmarks with the road stored in the GIS database. Then, each road will logically define a local map.

Figure 1 Example of roads stored in a GIS layer (NavTeQ database-Benomad rendering)



The road layer information is provided by cartographers for route guidance purposes. Road layer information is summarised in Table 1.

Table 1 Road layer information in a GIS

<i>Road map layer</i>
<ul style="list-style-type: none"> • Fine road connectedness • Coarse road geometry • Attributes: <ul style="list-style-type: none"> – Driving direction – Speed limit – Road ID – Postal boundaries – Date of data acquisition • Points of interest

2.2 Landmarks for precise localisation

For precise navigation, exteroceptive landmarks are necessary. There are different kinds of landmarks that depend on the particular sensors being used. They can be classified in the following categories.

Active landmarks: active landmarks are beacons that contain active components in order to transmit a signal. They mainly rely on the use of radio-frequency signals (GPS pseudolites, transponders beneath the road surface, WiFi antennae, etc.). Such landmarks are usually distinguishable from each other. In this case, sensors are receivers equipped with an antenna.

Passive landmarks: they are artificial landmarks pertinently located in the environment for localisation purposes. Passive landmarks include magnets in the pavement and reflectors on roadside posts indicating bends.

Natural landmarks: natural landmarks are features of the environment detected by onboard sensors like video cameras or laser scanners (Howard et al., 2004; Weiss et al., 2005). They can correspond to characteristic points (edges of windows for instance), road markings, roofs of buildings, posts, curbs, sidewalks, etc.

Let us consider, for instance, visual landmarks with characteristic points (3D points – Royer et al., 2005 – or 2D points – Remazeilles et al., 2004) for the navigation of a Cycab using a mono-camera at video rate. These landmarks are characteristic points in images called Harris points (Harris and Stephens, 1988). Using these points it is possible to reconstruct the 3D pose (position and attitude) of the vehicle using a sequence of images in which each landmark has been detected at least in two images. These landmarks can be managed in a GIS by georeferencing the position of the camera (Jabbour et al., 2006).

Another approach consists in localising the landmarks in the same coordinate frame as the road map. These landmarks can be complex features like image-based planes (Benhimane and Malis, 2004) or sidewalk edges. Sidewalk edges are considered in the following.

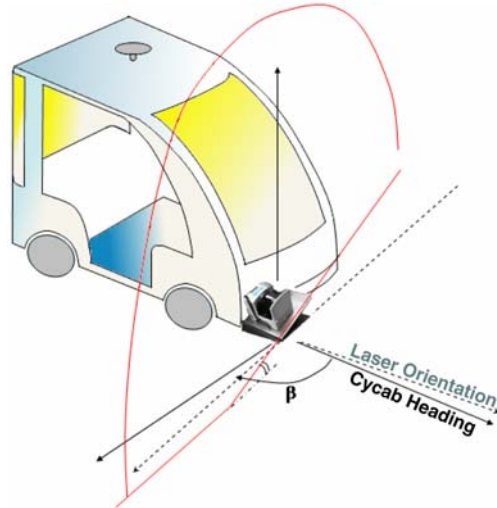
2.3 Sidewalk edge landmarks

GPS satellite signals are often blocked in urban areas. In such a situation, a localisation system can use DR sensors to maintain an estimate of the vehicle's pose. It is known that lateral drift is greater than longitudinal drift (Kelly, 2004). Therefore, the laser scanner has to be used to detect as many lateral landmarks as possible. Since the sidewalks and the façades of buildings naturally possess this lateral feature in urban areas, we propose using a laser scanner installed vertically (see Figure 2). A mirror can be installed to reflect the upper part of the beam in order to ensure collision avoidance, for instance. The horizontal and inclined setting proposed in Wijesoma et al. (2004) for road-boundary detection is an alternative.

The laser signal is first used to detect a pattern corresponding to a sidewalk edge. Our algorithm is based on the detection of the slope variation of successive segments of the telemeter frame. The first value of the slope that is higher than a threshold corresponds to the edge of the sidewalk. In Wijesoma et al. (2004) an extended Kalman filter is used to detect breaks in the laser signal in order to detect and compute the distance to the sidewalk edge. A prediction step is performed using the last two distances of the laser beam to predict the following one, then, if the innovation between the predicted distance and the measure is higher than a threshold, the corresponding point is

considered to be the sidewalk edge. In Adams et al. (2004) the same strategy is adopted using an Unscented Kalman Filter (UKF). From the real-time implementation point of view, a compromise between low-level and high-level computations has to be found. We believe that it is better to develop effective low-level methods and to find high-level localisation methods that are robust with respect to aberrant data.

Figure 2 A cybercar equipped with a vertical laser scanner (SICK LMS)



2.4 Enhanced geographical information layer

In general, an Enhanced Geographical Information Layer (EGIL) contains information relative to the environment detected by exteroceptive sensors. In our particular case, the EGIL contains sidewalk features detected by the laser scanner.

Storing all sidewalk landmarks would imply a large amount of data and consequently a huge amount of disk-space, which is unrealistic for real-time applications. In addition, on future itineraries the vehicle may not detect exactly the same landmarks. Therefore, the information has to be segmented, in the same way as for the road maps. To do this, a split and merge algorithm similar to the one in Borges and Aldon (2000) can be used (see Figure 3). Therefore, the EGIL information contains *nodes* describing the geometric nature of the landmarks and *connections* describing their topology.

In robotics, the management of map uncertainties is often important, especially for the approaches that follow the SLAM paradigm (Simultaneous Localisation and Map Building) (Dissanayake et al., 2001).

We propose to model the uncertainties of these two components.

The observation equations of each point I of the sidewalk (see Figure 7) are non-linear with respect to the vehicle pose X_v and the laser distance Y to the sidewalk point. Given the assumption of uncorrelated measurements, the imprecision in the position of the nodes can be obtained by propagating the covariance of the pose estimated error using a first-order Taylor expansion:

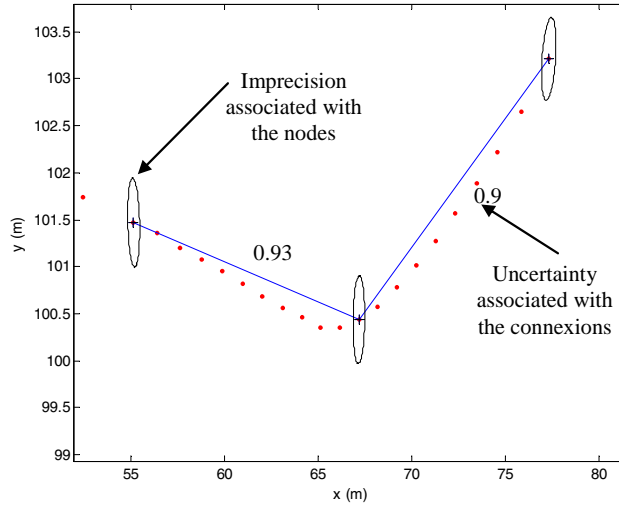
$$\begin{pmatrix} x_i \\ y_i \end{pmatrix} = h(X_v, Y) \quad (1)$$

Assuming also that the vectors X_v and Y are uncorrelated, the imprecision can be estimated by:

$$\text{var} \begin{pmatrix} x_i \\ y_i \end{pmatrix} = P_I = \frac{\partial h}{\partial X_v} P_v \frac{\partial h^T}{\partial X_v} + \frac{\partial h}{\partial Y} R \frac{\partial h^T}{\partial Y} \quad (2)$$

where P_v is the car's covariance matrix and R is the observation covariance.

Figure 3 Enhanced map with associated imprecision and uncertainty



The likelihood of the topological connections between the nodes also needs to be quantified since the sidewalk edge detection can be mistaken. Moreover, an urban environment is not a perfectly static environment: cars can be parked between the pavement and the cybercar. These vehicles may subsequently be removed, which will make the pavement reappear. In order to deal with these problems, a belief value can be associated with each segment of the map. The quantification of this uncertainty can rely on heuristic considerations as long as the result is in the interval $[0, 1]$ (Jabbour and Bonnifait, 2006). Using this formalism, regions without a sidewalk and regions containing parked cars are treated alike: a null belief of existence is associated with them.

3 Coarse localisation

One way of managing natural landmarks is to have map-matched estimates of the pose of the vehicle, even if these estimates are inaccurate.

In urban areas, GPS suffers from several drawbacks such as multitracks and masking: GPS signals are often blocked or reflected by high-rise buildings. Because a vehicle cannot be localised continuously by GPS alone, localisation involves merging data from an odometer, a gyrometer, GPS and map information. If the signal from GPS satellites is blocked by buildings, for example, the evolution model provides a DR estimate, whose drift may be corrected using the map information.

In order to simplify the matching process, which is a difficult task because of the offset that always exists between the road map and the GPS frame, we assume that the

vehicle follows the precomputed itinerary chosen by the user and obtained from the route-planning feature of the GIS. Figure 4 gives an example of a precomputed itinerary in an urban area.

Figure 4 Planned itinerary of the vehicle plotted in bold



The coarse localisation is done by a pose tracking method based on Kalman filtering. The DR sensors are used in a prediction stage, which is corrected, by GPS, if it is available and coherent (no multitracks), and the map. The fusion is done by Kalman Filtering – Extended Kalman Filtering (EKF) here, but it could be UKF, which uses a prediction/update mechanism.

3.1 DR prediction

The mobile frame is chosen with its origin at the centre of the rear axle. The x -axis is aligned with the longitudinal axle of the cybercar. The vehicle's position is represented by (x_k, y_k) , the Cartesian coordinates of M in a global frame (a projection of geographic data). The bearing angle is denoted θ_k .

The evolution model of the vehicle is non-linear:

$$X_{v,k+1} = f(X_{v,k}, U_{v,k}, \gamma_k) + \alpha_{v,k} \quad (3)$$

where $X_{v,k}$ is the vehicle state vector at instant k , composed of (x_k, y_k, θ_k) , $U_{v,k}$ the vector of the measured inputs consisting of (Δ_k, w_k) , Δ_k and w_k being respectively the elementary distance covered by the rear wheels and the elementary rotation of the mobile frame. $\alpha_{v,k}$ is the process noise and γ_k represents the measurement error of the inputs. $\alpha_{v,k}$ and γ_k are assumed to be uncorrelated and with zero mean noise.

If the road is perfectly planar and horizontal, and if the motion is locally circular, the evolution model can be expressed by:

$$\begin{cases} x_{v,k+1} = x_{v,k} + \Delta_k \cos\left(\theta_{v,k} + \frac{w_k}{2}\right) \\ y_{v,k+1} = y_{v,k} + \Delta_k \sin\left(\theta_{v,k} + \frac{w_k}{2}\right) \\ \theta_{v,k+1} = \theta_{v,k} + w_k \end{cases} \quad (4)$$

The values of Δ_k and w_k are computed using the odometer measurements of the rear wheels and a fibre optic gyrometer.

In the prediction step, the cybercar evolves using (2) and the covariance of the error is estimated.

3.2 GPS correction

When a GPS position is available, a correction of the predicted pose is performed. In urban areas, GPS suffers from multitracks and bad satellite constellations (urban canyoning) that degrade the position that it delivers. So, when a GPS position is available, it is necessary to verify its coherence. To this end the Normalised Innovation Squared (NIS) with a chi-square distribution is used: a distance d_m is computed between the GPS observation and the state vector.

Let Y_v be the GPS observation vector, μ_v the innovation vector.

$$Y_v = \begin{bmatrix} x_{\text{GPS}} \\ y_{\text{GPS}} \end{bmatrix} = \begin{bmatrix} 1 & 0 & 0 \\ 0 & 1 & 0 \end{bmatrix} X_v + \beta_{\text{GPS}} = C_v X_v + \beta_{\text{GPS}} \quad (5)$$

$$\mu_v = \begin{bmatrix} x_{\text{GPS}} - x \\ y_{\text{GPS}} - y \end{bmatrix} \quad (6)$$

$$d_m = \mu_v (P_\mu)^{-1} \mu_v^T \quad (7)$$

where (x, y) is the predicted position and P_μ is the covariance of the innovation.

If the computed distance d_m is smaller than a threshold, for instance $\chi^2(0.05, 3)$, then the GPS measurement is assumed to be correct and a correction of the predicted pose is performed. Otherwise, the DR pose provided by the evolution model is retained. It should be noted that the GPS noise is not stationary. The GPS measurement error can be estimated in real time using the *NMEA* sentence *GST*. This information is provided by the TRIMBLE AGGPS132 GPS receiver used in the experiments.

3.3 Map correction

Before starting the localisation system, an itinerary is computed and we assume that the vehicle follows this path faithfully. Each segment in the GIS map has an Identifier (ID). This ID will be used in the following stages to perform the geo-referencing of the landmarks.

Let us consider the segment selection problem, which consists in extracting from the GIS map the most likely segment using the estimated state vector. The distances between the estimate and the nearest segments of the itinerary are computed. The segment that has

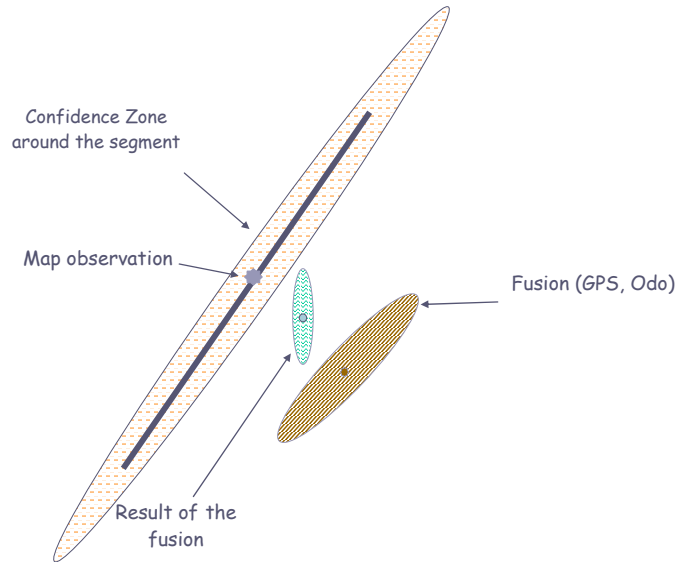
the smallest distance and whose driving direction corresponds to the orientation of the vehicle is taken to be the correct one. As we will see in Section 6, this simple matching strategy gives good results since the planned itinerary has no intersections. The matched point is obtained by projecting the estimated position onto the selected segment.

The matched point (see Figure 5) can be used as a map observation (denoted Y_{vm}) in order to correct the drift in the DR estimate if GPS is unavailable:

$$Y_{vm} = \begin{bmatrix} x_{MAP} \\ y_{MAP} \end{bmatrix} = \begin{bmatrix} 1 & 0 & 0 \\ 0 & 1 & 0 \end{bmatrix} X_v + \beta_{MAP} = C_v X_v + \beta_{MAP} \quad (8)$$

The covariance β_{MAP} associated with the map observation is taken to be proportional to the width of the road, and its major axis is parallel to the selected segment (El Badaoui El Najjar and Bonnifait, 2005). Another NIS coherence test is used to verify the map observation before fusing it as part of a Kalman filter correction stage.

Figure 5 Merging a segment with the previous estimated position



4 Detecting and geo-referencing landmarks

Before navigating autonomously, the EGIL of the GIS has to be created and initialised. In this stage, the cybercar is driven manually and the sensor measurements are timestamped and stored for post-processing.

The procedure for this modelling stage is as follows:

- identify where the vehicle must move autonomously
- compute the itinerary using the route calculation facility of GIS
- have a map of the road map
- drive the cybercar manually along this itinerary

- compute the coarse localisation
- build the map of sidewalks with associated uncertainties
- geo-reference this map in the GIS as an EGIL.

In subsequent itineraries these landmarks will be extracted each time the vehicle navigates in the same area.

One of the difficulties of this approach is the management and the structuring of the large amount of landmark data in the EGIL for online navigation. How may landmark information be organised for a cybercar that moves around in a large area containing many roads? The usual answer to this question is to group landmarks together in local maps, a local map being a set of landmarks put together because of

- 1 memory constraints arising from the use of embedded systems
- 2 the need to download or update a limited amount of data from a distant server
- 3 the connections that exist between the landmarks, essential for computing a location.

Consequently, we propose grouping the detected urban landmarks together in local maps to facilitate their management. For this purpose, the use of the ID of the roads defined in the GIS road map layer is well adapted for cybercars, since the robot uses the planned itinerary computed from the road map. Moreover, a road is a set of segments having the same ID, possibly with an intersection at its beginning or/and at its end. So, as long as the cybercar is navigating along the same road, it uses the same set of landmarks.

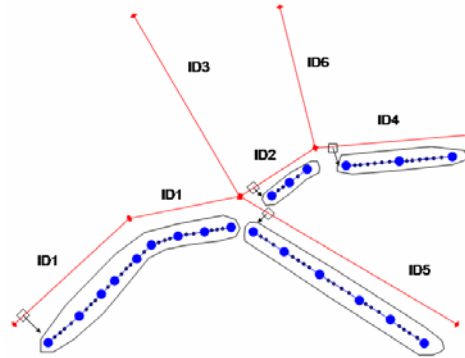
Furthermore, each road can be one-way or two-way (this information is contained in the road attributes). For one-way roads, a unique local map is built. It contains all the landmarks matched to it. For two-way roads, two maps are built, one for each direction: East To West (E2W) or West To East (W2E). If the road is parallel to the y -direction (North), the map is denoted E2W.

Finally, Table 2 describes the information associated with each local map.

Table 2 Laser landmarks with extended attributes for their management in the GIS

<i>Local map: map_j</i>
<ul style="list-style-type: none"> • GIS ID • Direction (E2W or W2E) • Set of I landmarks made up of <ul style="list-style-type: none"> – Coordinates of the segmented data – Covariance matrix of the error on the position of the nodes – Belief vector – Matched position $X_{map_{j,l}}$ – Date of data acquisition

Figure 6 illustrates the procedure. The dotted points correspond to detected side-walks, large blue points to segmented data, black polygons to local maps attached to the roads, whose GIS IDs are indicated by the 'IDxx' labels.

Figure 6 Vectoring and grouping landmark data in local maps

The creation and initialisation of the EGIL can be performed online. While moving, the laser scanner data is buffered with the corresponding road ID retrieved during the coarse localisation stage (Section 3). In parallel, the sidewalk detection algorithm is applied to localise the curb edges with their imprecision using the estimated covariance of the state of the vehicle. The beginning and the end of the curb are identified. When a road with a different ID is encountered, the buffered data is sent to the segmentation module that returns a segment or a set of connected segments with associated imprecision and accuracy (as shown in Figure 3).

5 Autonomous navigation

We now consider a vehicle navigating in a previously learnt environment. An itinerary will have been computed using the GIS road map layer. While the vehicle follows this precomputed itinerary, two localisation processes occur. The first takes place in the road map layer using coarse localisation, and the second uses landmarks for a precise localisation in order to control the movement of the vehicle as described in Benhimane and Malis (2004), Remazeilles et al. (2004) and Royer et al. (2005).

Landmark management for navigation consists in two parallel tasks:

- local map extraction
- landmark selection.

Once the right landmark has been extracted, the laser scanner data is used to correct the estimated pose.

5.1 Local map selection

The goal of this task is to obtain a vehicle position with metre-level precision and then to find the appropriate local landmark map stored in the GIS landmark layer. The localisation algorithm is the same as the one used in the learning stage: it merges GPS, DR sensors and road map information corresponding to the computed itinerary. Then, the road ID is retrieved and the driving direction (E2W or W2E) is deduced from the motion. This information enables the selection of the appropriate local map. If the selected local map no longer corresponds to the current local map, new landmarks are loaded into the vehicle memory.

This supervisory task is repeated during the navigation process. It guarantees correct transitions between two local maps.

5.2 Laser landmark extraction

This part deals with the extraction and use of the segmented laser features (sidewalk edges) within the previously selected local map map , which comprises a set of laser landmarks.

Let $(x_{pred}, y_{pred}, \theta_{pred})$ be the predicted pose. This allows the laser scanner reference position $(x_{T,pred}, y_{T,pred})$ to be estimated.

The equation for the line D which passes through $(x_{T,pred}, y_{T,pred})$ and which has $\tan(\theta_{pred} + \beta)$ as slope can be written as $y = sx + k$ (see Figure 7). We have the function

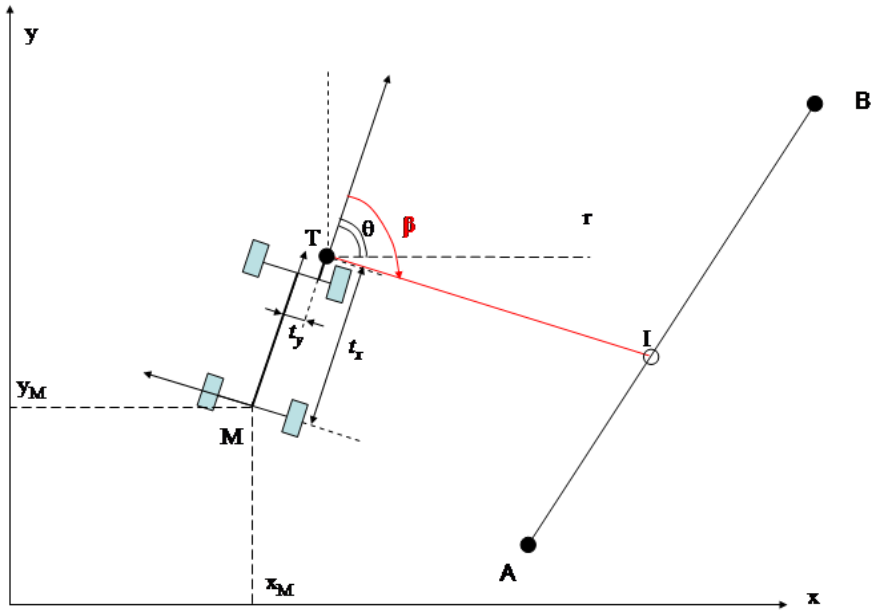
$$h(x, y) = y - sx - k \tag{9}$$

Line D intersects segment $[AB]$ only if

$$h(x_A, y_A)h(x_B, y_B) \leq 0 \tag{10}$$

To be a real sidewalk edge, the associated segment must also have a non-null belief of existence (higher than a threshold). If more than one segment satisfies these criteria, the nearest one is selected. As we will see in this simple matching strategy gives good results.

Figure 7 Observation model of the laser scanner



5.3 Pose updating using the laser scanner

If a curb is detected, the laser scanner can be used to correct the pose. Let us suppose here that the correct segment $[AB]$ has been selected from the enhanced map. The observation is the telemetric distance r to the sidewalk edge. r can be predicted by:

$$r_{\text{pred}} = \sqrt{(x_{\text{T}} - x_{\text{I}})^2 + (y_{\text{T}} - y_{\text{I}})^2} \quad (11)$$

where $(x_{\text{I}}, y_{\text{I}})$ is the predicted intersection point of the laser beam with segment $[AB]$ (see Figure 7).

The predicted distance r_{pred} is written as:

$$r_{\text{pred}} = \left| \frac{ax_{\text{pred}} - y_{\text{pred}} + b}{\sqrt{a^2 + 1} \cos(\theta_{\text{pred}} + \beta - \tan^{-1}(a) - (\pi/2))} \right| \quad (12)$$

where a and b are the parameters of the segment passing through points A and B . The distance r_{pred} is a non-linear function of the vehicle's predicted pose and of the coordinates of segment $[AB]$. It can be used in an EKF scheme to correct the estimated pose of the cybercar.

When a valid laser scanner observation is available, it is important to verify its coherence. The same NIS test applied on GPS and road map data is used here.

6 Experimental results

Real experiments were carried out with our experimental car in the downtown area of Compiègne using a KVH fibre optic gyro, an odometer input and an L1 GPS receiver (Trimble AgGPS 132) with geostationary differential correction (Satellite Based Augmentation System Omnistar).

A SICK LMS291 Laser Range Scanner at 75 Hz was used. We chose a 1° resolution and a range of 8.1 m. In this mode, the laser sends sentences of 181 values, each one corresponding to an angle varying from 0° to 180° in the laser range scanner frame. The GPS was set to a '3D only-mode' (position fix computable only if four satellites are visible). In order to obtain reliable positions the DOP threshold was set to a low value and the SNR threshold to a high value. This sort of tuning gives rise to a reliable but intermittent positioning in urban areas. The timestamped data was saved in order to analyse the results in post-processing and verify the extracted landmarks. The road map used was a standard NavTeQ database managed by a GIS developed using Benomad SDK (Software Development Kit – Labrousse, 2006).

In this section, the two localisation processes are studied: metre-level localisation in the road map layer using merged GPS and precise (decimetre-level) localisation using the laser landmarks.

6.1 Local map management

Figure 8 shows local maps associated with each road in the NavTeQ database. Each local map has its particular ID (blue squares). The precomputed itinerary is shown in red. Other road segments in the road map are plotted in dashed black. The arrows show the links between the laser local maps and the digital road database. The offset of the NavTeQ database is particularly visible in this experiment. Its value in this part of the urban area is 12 m North and 8 m East.

Figure 8 Local maps associated with the road database after the learning stage (each local map has its own colour; for colours see online version)

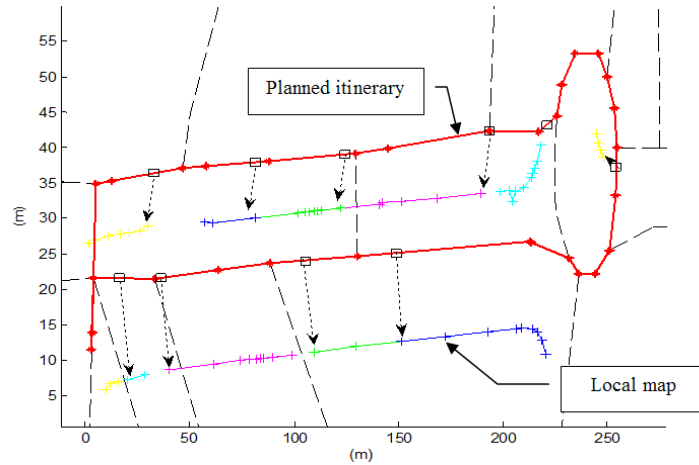
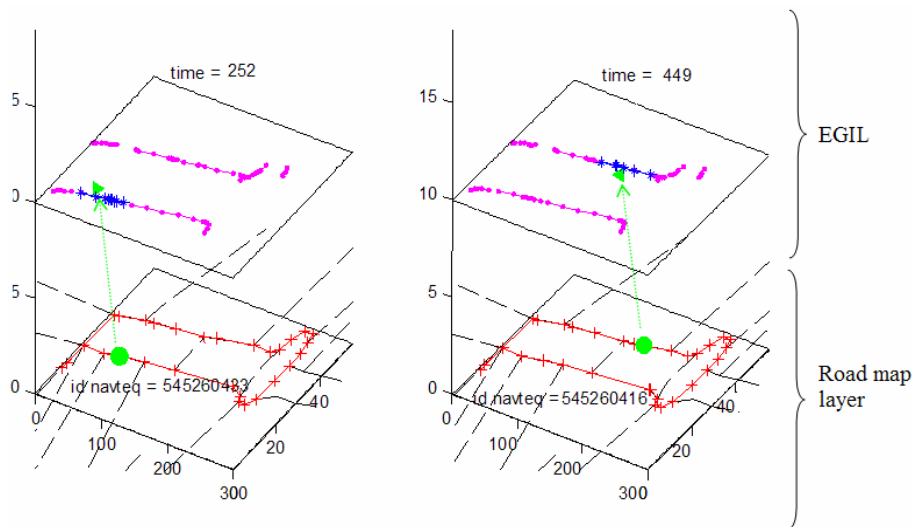


Figure 9 shows the local map extraction process at two different points in the same navigation stage. The precomputed itinerary of the cybercar is plotted in red in the bottom layer corresponding to the road map layer. The other road segments are plotted in dashed black. The upper part represents the enhanced maps layer. The green triangle indicates the merged vehicle position in the precise map, and the green circle represents the map-matched position used to extract the local feature map, which is shown in blue in the enhanced layer. It will be remarked that some roads may have no associated local map, if there is no sidewalk or if the sidewalk edge has not been detected. This is the case in the gyratory area: there is no sidewalk each time there is an exit road. Moreover, the detection algorithm has missed two short and curved parts of the gyratory sidewalk, as can be seen in the enhanced maps layer of Figure 9.

Figure 9 Local map extraction at two points in the navigation stage (for colours see online version)



6.2 Precise localisation using the landmarks

The geometry of the enhanced maps is more detailed and the localisation therefore more precise. A Post Processed Kinematic (PPK) GPS receiver (a Trimble 5700 dual-frequencies L1/L2) was used to compute estimation errors using an offline software package Trimble Total Control (TTC). A test area with good satellite visibility was chosen, since a well-functioning PPK needs at least five satellites. One way of evaluating the precision of the reference is to study the values of the L1 pseudo-range residuals (phase measurements). For the experiments reported in this paper, we verified that the pseudo-range residuals were in the order of few centimeters as shown in Figure 10. Other than between 09:58 and 10:00, where at least one phase ambiguity was not correctly fixed (giving rise to a horizontal error of up to ~5 cm), the residuals are very small, indicating a high level of precision.

Figure 10 L1 PPK residuals obtained with TTC versus time: the time of the trial is indicated by the wide (orange) bar (for colours see online version)

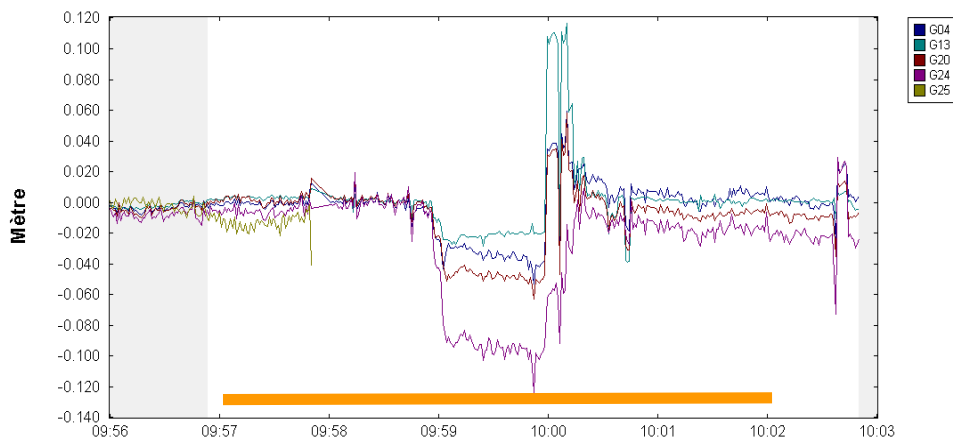


Figure 11 shows lateral localisation errors in a Frenet's frame. GPS masks were artificially introduced by eliminating several parts of the AgGPS 132 data in order to reproduce urban canyons. The average duration of the GPS masking was about 21 sec; with an average covered distance of 170 m during each GPS outage. The grey bars show the GPS-L1 outages. The thin line represents the errors (in metres) of a localisation algorithm using only GPS coupled with DR sensors, while the bold line represents the localisation error of the complete system that fuses GPS, DR sensors and extracted segments from local maps. The lateral error rarely exceeds 1 m, while the GPS+DR algorithm can drift significantly during GPS outages.

Figure 12 plots x and y errors for both algorithms with 3σ estimated contours (thin blue lines). The longitudinal error is consistent with the localisation process, while the lateral error is not wholly consistent. The same phenomenon has been observed in Castellanos et al. (2004) and is often due to an EKF-Based algorithm that is sensitive to large errors because of the linearisation of the equations.

Figure 11 Lateral localisation errors with and without the use of the local maps

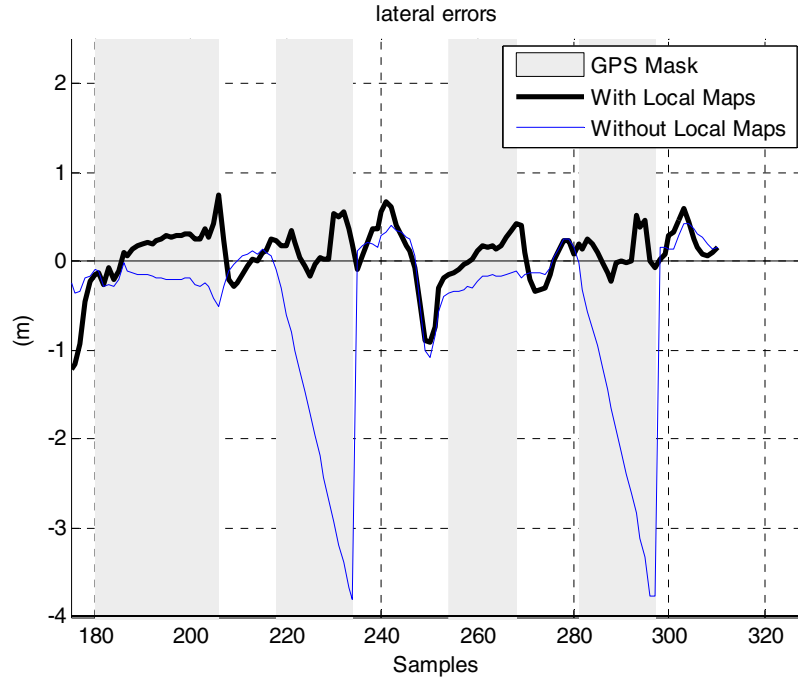
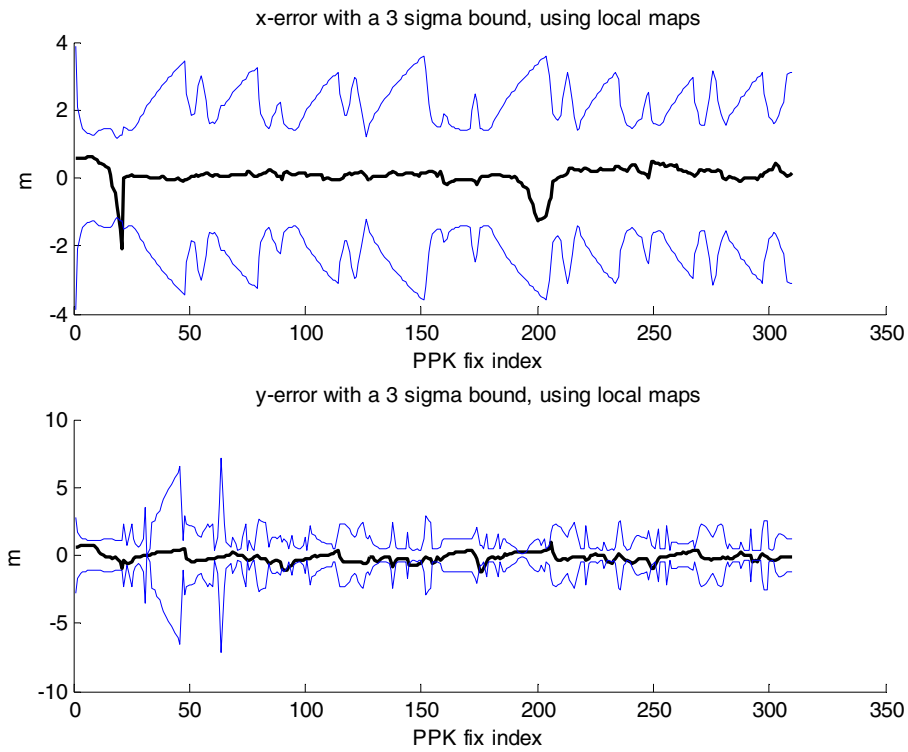


Figure 12 x and y errors with the 3σ estimated bound



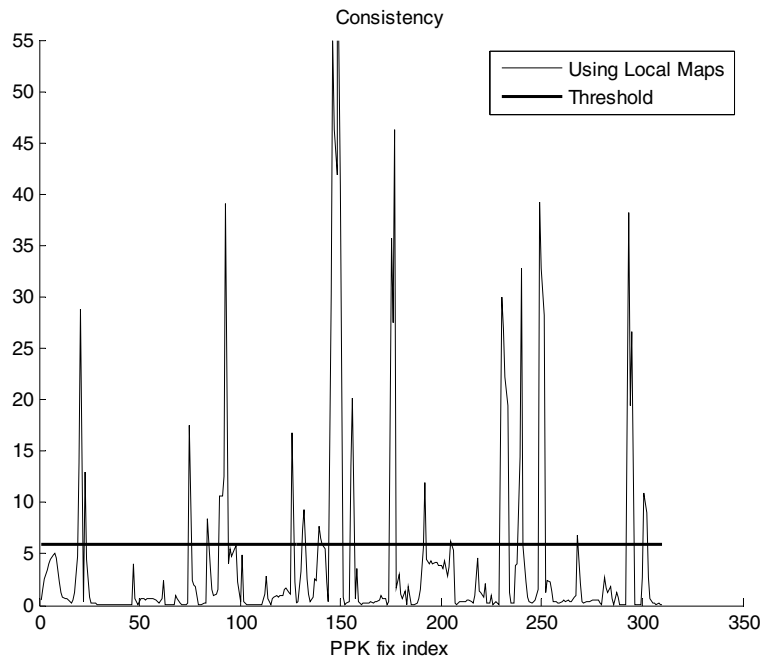
In order to evaluate more precisely the consistency of the localisation system, the Normalised Estimation Error Squared (NEES) was computed using:

$$D^2 = \begin{pmatrix} \hat{x} - x_{ppk} \\ \hat{y} - y_{ppk} \end{pmatrix}^T \cdot P_{xy}^{-1} \cdot \begin{pmatrix} \hat{x} - x_{ppk} \\ \hat{y} - y_{ppk} \end{pmatrix} \quad (13)$$

Consistency is checked by using a chi-squared test, for instance $D^2 < \chi^2(0.05, 2)$.

Figure 13 shows the consistency of the estimated vehicle position throughout the test. The localisation consistency is 88.4% rather than 95%, since a $\chi^2(0.05, 2)$ law was used. This small difference indicates a good behaviour and a good tuning of the filter. Therefore, we believe that the estimated covariance represents correctly the confidence in the localisation. A lateral error smaller than the longitudinal error is to be expected, owing to the laser scanner installation on board the vehicle: lateral features are used to correct the lateral drift. From the control point of view, it is an interesting feature since lateral precision is essential for good trajectory tracking.

Figure 13 Consistency of the estimated vehicle location $\chi^2(0.05, 2)$



7 Conclusion

This paper proposes a method for managing a particularly large quantity of landmark data in a GIS for precise localisation in urban areas. The example of laser landmarks is considered. The method is illustrated with real experiments carried out in the downtown area of Compiègne, France.

Our proposition is to gather landmarks in local enhanced maps characterised by a coarse localisation process performed using a road map layer, an L1-GPS receiver and

odometry. This localisation process can be interpreted as symbolic localisation, since its main output is the ID of the road and the driving direction. In order to simplify the map-matching process, an itinerary obtained from the route calculation of the GIS software is used. This itinerary has to be strictly followed by the vehicle during the learning and navigation stages. In the work presented here, a local map is a set of segments representing the sidewalk edges and having the same IDs as the road stored in the GIS road map layer. For two-way roads, two maps can be associated with the same road, one for each direction. Experimental results indicate that this approach is a good candidate for the management of landmarks in urban areas, since landmarks stored in a previous passage can be correctly extracted, although a large offset can occur between the map and the GPS data.

Once the local map has been retrieved, a precise localisation is obtained using the natural landmarks detected by the laser scanner. As shown by the experiments, the absolute lateral precision obtained with our laser scanner installation is better 50 cm. We do not believe that this error rules out autonomous navigation, so long as the cybercar can follow approximately the same trajectory as in the learning stage. In this case, repeatability is more important than precision, and easier to obtain thanks to the use of local landmarks.

Acknowledgement

This research was carried out within the framework of the Mobivip project, part of the third French PREDIT programme from January 2004 to December 2006.

References

- Adams, M., Zhang, S. and Xie, L. (2004) 'Particle filter based outdoor robot localization using natural features extracted from laser scanners', *Proceedings of the 2004 IEEE International Conference on Robotics and Automation (ICRA)*, New Orleans, LA.
- Benhimane, S. and Malis, E. (2004) 'Real-time image-based tracking of planes using efficient second-order minimization', *IEEE/RSJ International Conference on Intelligent Robots Systems*, Sendai, Japan.
- Borges, G. and Aldon, M.-J. (2000) 'A split-and-merge segmentation algorithm for line extraction in 2-D range images', *International Conference on Pattern Recognition (ICPR'00)*, 3–8 September 2000, Barcelona, Spain.
- Castellanos, J.A., Neira, J. and Tardos, J.D. (2004) 'Limits to the consistency of EKF-based SLAM', *Proceedings of the International Symposium on Intelligent Autonomous Vehicles*, Lisbon, Portugal.
- Dissanayake, M.W.M.G., Newman, P., Clark, S., Durrant-Whyte, H.F. and Csorba, M. (2001) 'A solution to the simultaneous localization and map building (SLAM) problem', *IEEE Transactions on Robotics and Automation*, Vol. 17, No. 3, pp.229–241.
- El Badaoui El Najjar, M. and Bonnifait, P. (2005) 'A road-matching method for precise vehicle localization using Kalman filtering and belief theory', *Journal of Autonomous Robots*, Vol. 19, No. 2, pp.173–191.
- Georgiev, A. and Allen, P.K. (2004) 'Localization methods for a mobile robot in urban environments', *IEEE Transactions on Robotics and Automation*, Vol. 20, No. 5, pp.851–864.

- Harris, C. and Stephens, M. (1988) 'A combined corner and edge detector', *Proceedings of the Fourth Alvey Vision Conference*, Manchester, UK, pp.147–151.
- Howard, A., Wolf, D. and Sukhatme, G. (2004) 'Towards 3D mapping in large urban environments', *Proceedings of 2004 IEEE/RSJ International Conference on Intelligent Robots and Systems*, 28 September–2 October, Sendai, Japan.
- Jabbour, M. and Bonnifait, P. (2006) 'Global localization robust to GPS outages using a vertical ladar', *The 9th IEEE International Conference on Control, Automation, Robotics and Vision, ICARCV 06*, 5–8 December 2006, Singapore.
- Jabbour, M., Cherfaoui, V. and Bonnifait, P. (2006) 'Management of landmarks in a GIS for an enhanced localisation in urban areas', *IEEE Intelligent Vehicle Symposium 2006*, Tokyo, Japan, 13–15 June.
- Kais, M., Dauvillier, S., De La Fortelle, A., Masaki, I. and Laugier, C. (2004) 'Towards outdoor localization using GIS, vision system and stochastic error propagation', *International Conference on Autonomous Robots and Agents ICARA*, December, Palmerston North, New Zealand.
- Kelly, A. (2004) 'Linearized error propagation in odometry', *The International Journal of Robotics Research*, Vol. 23, No. 2.
- Kim, Y., Pyeon, M. and Eo, Y. (2000) 'Development of hypermap database for ITS and GIS', *Computers, Environment and Urban Systems*, Vol. 24, pp.45–60.
- Labrousse, D. (2006) 'Benomad SDK', Available at: www.benomad.com.
- Parent, M. and Gallais, G. (2002) 'Intelligent transportation in cities with CTS', *ITS World Congress*, October, Chicago.
- Remazeilles, A., Chaumette, F. and Gros, P. (2004) 'Robot motion control from a visual memory', *IEEE International Conference on Robotics and Automation, ICRA'04*, Vol. 4, New Orleans, Louisiane, April, pp.4695–4700.
- Royer, E., Bom, J., Dhome, M., Thuillot, B., Lhuillier, M. and Marmouton, F. (2005) 'Outdoor autonomous navigation using monocular vision', *IEEE/RSJ International Conference on Intelligent Robots and Systems*, Edmonton, Canada, August, pp.3395–3400.
- Vasquez, D., Large, F., Fraichard, T. and Laugier, C. (2004) 'High-speed autonomous navigation with motion prediction for unknown moving obstacles', *Proceedings of the IEEE/RSJ International Conference on Intelligent Robots and Systems (IROS)*, Sendai (JP), October.
- Wang, D., Low, C., He, B. and Pham, M. (2004) *Accurate Positioning for Real-Time Control Purpose: Integration of GPS, NAV200 and Encoder Data*, ICARCV.
- Weiss, T., Kaempchen, N. and Dietmayer, K. (2005) 'Precise ego-localization in urban areas using laser scanner and high accuracy feature maps', *IEEE Intelligent Vehicle Symposium*, Las Vegas, USA, 6–8 June.
- Wijesoma, W.S., Kodagoda, K.R.S. and Balasuriya, A. (2004) 'Road-boundary detection and tracking using Ladar sensing', *IEEE Transactions on Robotics and Automation*, Vol. 20, No. 3, pp.456–464.